Arctic Ocean Primary Productivity: The Response of Marine Algae to Climate Warming and Sea Ice Decline

K. E. Frey[1], J. C. Comiso[2], L. W. Cooper[3], J. M. Grebmeier[3], L. V. Stock[2]

[1]Graduate School of Geography, Clark University, Worcester, Massachusetts, USA
[2]Cryospheric Sciences Laboratory, NASA Goddard Space Flight Center, Greenbelt, MD, USA
[3]Chesapeake Biological Laboratory, University of Maryland Center for Environmental Science, Solomons, MD, USA

Highlights

- Satellite estimates of ocean primary productivity (i.e., the rate at which marine algae transform dissolved inorganic carbon into organic material) showed higher values for 2020 (relative to the 2003–2019 mean) for seven of the nine investigated regions (with the Sea of Okhotsk and Bering Sea showing the lower than average values).
- All regions continue to exhibit positive trends over the 2003–2020 period, with the strongest trends in the Eurasian Arctic, Barents Sea, and Greenland Sea.
- During July and August 2020, a ~600 km long region in the Laptev Sea of the Eurasian Arctic showed much higher chlorophyll-*a* concentrations (~2 times higher for July and ~6 times higher for August) than the same months of the multiyear average (2003–2019), associated with continual declines of sea ice throughout the region.

Autotrophic single-celled algae living in sea ice (ice algae) and water column (phytoplankton) are the main primary producers in the Arctic Ocean. Through photosynthesis, they transform dissolved inorganic carbon into organic material. Consequently, primary production provides a key ecosystem service by providing energy to the entire food web in the oceans. Primary productivity is strongly dependent upon light availability and the presence of nutrients, and thus is highly seasonal in the Arctic. In particular, the melting and retreat of sea ice during spring are strong drivers of primary production in the Arctic Ocean and its adjacent shelf seas, owing to enhanced light availability and stratification (Barber et al. 2015, Leu et al. 2015, Ardyna et al. 2017). Recent studies have emphasized that primary production occurs under lower light conditions and earlier in the seasonal cycle than previously recognized (Randeloff et al. 2020). Other recent studies also suggest that increased nutrient supply may also influence overall production (Henley et al. 2020; Lewis et al. 2020). Regardless, recent declines in Arctic sea ice extent (see the essay on *Sea Ice*) have contributed substantially to shifts in primary productivity throughout the Arctic Ocean. However, the response of primary production to sea ice loss has been both seasonally and spatially variable (e.g., Tremblay et al. 2015, Hill et al. 2018).

Here we present satellite-based estimates of algal chlorophyll-*a* (occurring in all species of phytoplankton), based on ocean color, and subsequently provide calculated primary production estimates. These results are shown for ocean areas with less than 10% sea ice concentration and, therefore, do not include production by sea ice algae or under-ice phytoplankton blooms, which can be significant (e.g., Lalande et al., 2019).

Chlorophyll-*a*

Measurements of the algal pigment chlorophyll (e.g., chlorophyll-*a*) serve as a proxy for the amount of algal biomass present (e.g., Behrenfeld and Boss, 2006) as well as overall plant health. The complete, updated MODIS-Aqua satellite chlorophyll-*a* record for the northern polar region for the years 2003–2020 serve as a time-series against which individual years can be compared. For this reporting, we show mean monthly chlorophyll-*a* concentrations calculated as a percentage of the 2003–2019 average, which was chosen as the reference period in order to maximize the length of the satellite-based time series.

The color-coded monthly 2020 data presented in **Fig. 1** show a distribution of the ratio of chlorophyll-*a* concentrations and the multiyear average of data from 2003 to 2019 expressed as percentages, where patterns are spatially and temporally heterogeneous across the Arctic Ocean. These patterns are often associated with the timing of the seasonal break-up and retreat of the sea ice cover (**Fig. 2**): high percentages tend to occur in regions where the break-up is relatively early, while low percentages tend to occur in regions where the break-up is delayed. The most notable enhanced values in 2020 occurred during July and August, with high concentrations of chlorophyll-*a* occurring in the Laptev Sea of the Eurasian Arctic (**Figs. 1c** and **1d**). In particular, this regional increase in chlorophyll-*a* concentrations extended ~600 km in length and exhibited on average ~2 times higher (July) and ~6 times higher (August) concentrations than previous years on record. Additional widespread increases in chlorophyll-*a* concentrations occurred along the ice edge in the Greenland Sea during May and June (**Figs. 1a** and **1b**) associated with increases in sea ice to the west (**Figs. 2a** and **2b**), as well as in the Barents Sea during May (**Fig. 1a**). Some of the lowest percentages of chlorophyll-*a* concentrations (i.e., low primary productivity) occurred in the northern Bering Sea during May, June, and August (**Figs. 1a**, **1b**, and **1d**) and in the Barents Sea in June, July, and August (**Fig. 1b**, **1c**, and **1d**).

As noted above, some of the lowest percentages of chlorophyll-*a* concentrations observed in 2020 occurred over the shelf region of the Bering Sea during May, June, and August (**Figs. 1a**, **1b**, and **1d**). During June, these low percentages extended northward through the Bering Strait and onto the Chukchi Shelf (**Fig. 1b**). It is unclear from the satellite time series what role sea ice may be playing in these reductions of chlorophyll-*a* concentrations: 2020 experienced a resurgence of seasonal sea ice cover across the northern Bering Sea and Bering Strait region (e.g., **Fig. 2a**) compared to drastic reductions observed in 2018 (Frey et al., 2018; Stabeno and Bell, 2019) and 2019 (Frey et al., 2019), yet chlorophyll-*a* concentrations in the region do not appear to respond in a consistent way to these potential sea ice forcings. In general, having knowledge of how regions experience changes in chlorophyll-*a* concentrations alongside dramatic losses of sea ice cover provides insight into what to expect with future sea ice declines. However, while many of these observed patterns are directly linked to sea ice variability (and therefore light availability), it is important to note that there are other dominant factors at play that add to the complexity of observed chlorophyll-*a* concentrations such as the distribution and availability of nutrients (e.g., Giesbrecht et al., 2019; Lewis et al., 2020). The impacts of sea ice decline on specific water column phytoplankton properties, such as community composition and carbon biomass (Neeley et al, 2018), as well as broader ecosystem responses (Duffy-Anderson et al., 2019) will also be critical to continue to monitor. Furthermore, it is important to reiterate that the satellite ocean color data do not account for early-season under-ice blooms that may contribute substantially to primary productivity in these regions (e.g., Arrigo et al., 2012).

Deployment of a new sediment trap array in the northern Bering Sea, together with a mooring array in fall 2020 should improve understanding of seasonal carbon production and export in this region, just as new year-round results reported from the Chukchi Ecsosytem Observatory in the northern Chukchi Sea (Lalande et al., 2020) have improved understanding of annual production.

Primary Production

Chlorophyll-*a* concentrations give an estimate of the total standing stock of algal biomass. However, rates of primary production (i.e., the production of organic carbon via photosynthesis) provide a different perspective since not all algae present in the water column are necessarily actively producing, and can be estimated by combining remotely sensed chlorophyll-*a* concentrations with sea surface temperatures, incident solar irradiance, and mixed layer depths (see caption in **Fig. 3** for references to details of the method for estimation). Estimates of ocean primary productivity for nine regions (and the average of these nine regions) across the Arctic (relative to the 2003–2019 reference period) were assessed (**Fig. 3**, **Table 1**). In particular, the Eurasian Arctic designation includes the Kara Sea, Laptev Sea, and East Siberian Sea, whereas the Amerasian Arctic designation includes the Chukchi Sea, Beaufort Sea, and Canadian Archipelago region. Our results show above average primary productivity for 2020 in all regions except for the Sea of Okhotsk and Bering Sea (**Fig. 3**, **Table 1**). In the longer term, positive trends in primary productivity occurred in all regions during the period 2003–2020 (**Fig. 3**, **Table 1**). Statistically significant positive trends occurred in the Eurasian Arctic, Barents Sea, Greenland Sea, Hudson Bay, Baffin Bay/Labrador Sea, North Atlantic, and for the average of the nine regions. The steepest trends over the 2003–2020 period were found for the Eurasian Arctic (12.90 g C/m^2/yr/decade, or a ~37.9% increase), the Barents Sea (8.97 g C/m^2/yr/decade, or a ~20.1% increase), and the Greenland Sea (6.39 g C/m^2/yr/decade, or a ~18.8% increase).

Acknowledgements

K. Frey would like to acknowledge financial support by the National Science Foundation Arctic Observing Network (AON) Program (Grants 1702137 and 1917434).

References

Ardyna, M., Babin, M., Devred, E., Forest, A., Gosselin, M., Raimbault, P. and Tremblay, J.-É., 2017: Shelf-basin gradients shape ecological phytoplankton niches and community composition in the coastal Arctic Ocean (Beaufort Sea). *Limnol. Oceanogr.*, 62, 2113–2132. doi:10.1002/lno.10554.

Arrigo, K. R., D. K. Perovich, R. S. Pickart, Z. W. Brown, G. L. van Dijken, K. E. Lowry, M. M. Mills, M. A. Palmer, W. M. Balch, F. Bahr, N. R. Bates, C. Benitez-Nelson, B. Bowler, E. Brownlee, J. K. Ehn, K. E. Frey, R. Garley, S. R. Laney, L. Lubelczyk, J. Mathis, A. Matsuoka, B. G. Mitchell, G. W. K. Moore, E. Ortega-Retuerta, S. Pal, C. M. Polashenski, R. A. Reynolds, B. Scheiber, H. M. Sosik, M. Stephens & J. H. Swift. 2012: Massive phytoplankton blooms under Arctic sea ice. *Science*, 336, 1408, doi:10.1126/science.1215065.

Barber, D. G., H. Hop, C. J. Mundy, B. Else, I. A. Dmitrenko, J. -É. Tremblay, J. K. Ehn, P. Assmy, M. Daase, L. M. Candlish, and S. Rysgaard. 2015: Selected physical, biological and biogeochemical implications of a rapidly changing Arctic Marginal Ice Zone. *Prog. Oceanogr.*, doi:10.1016/j.pocean.2015.09.003.

Behrenfeld, M. J., and E. Boss, 2006: Beam attenuation and chlorophyll concentration as alternative optical indices of phytoplankton biomass. *J. Mar. Res.*, 64, 431-451.

Behrenfeld, M. J., and P. G. Falkowski, 1997: Photosynthetic rates derived from satellite-based chlorophyll concentration. *Limnol. and Oceanogr.*, 42(1), 1–20.

Comiso, J. C., 2015: Variability and trends of the Global Sea Ice Covers and Sea Levels: Effects on Physicochemical Parameters. *Climate and Fresh Water Toxins*, Luis M. Botana, M. Carmen Lauzao and Natalia Vilarino, Eds., De Gruyter, Berlin, Germany.

Comiso, J. C., R. Gersten, and L. Stock, J. Turner, G. Perez, and K. Cho, 2017a: Positive trends in the Antarctic sea ice cover and associated changes in surface temperature, *J. Clim.*, 30, 2251–2267, doi:10.1175/JCLI-D-0408.1.

Comiso, J. C., W. N. Meier, and R. Gersten, 2017b: Variability and trends in the Arctic Sea ice cover: Results from different techniques, *J. Geophys. Res. Oceans*, 122, 6883–6900, doi: 10.1002/2017JC012768.

Duffy-Anderson, J. T., P. Stabeno, A. G. Andrews III, K. Cieciel, A. Dreary, E. Farley, C. Fugate, C. Harpold, R. Heintz, D. Kimmel, K. Kuletz, J. Lamb, M. Paquin, S. Porter, L. Rogers, A. Spear and E. Yasumiishi, 2019: Responses of the Northern Bering Sea and Southeastern Bering Sea Pelagic Ecosystems Following Record-Breaking Low Winter Sea Ice. *Geophys. Res. Lett.*, *46*. https://doi.org/10.1029/2019GL083396.

Frey, K. E., J. C. Comiso, L. W. Cooper, J. M. Grebmeier and L. V. Stock, 2018: Arctic Ocean Primary Productivity: The response of marine algae to climate warming and sea ice decline. In: [Arctic Report Card 2018], https://arctic.noaa.gov/Report-Card/Report-Card-2018/ArtMID/7878/ArticleID/778/Arctic-Ocean-Primary-Productivity-The-Response-of-Marine-Algae-to-Climate-Warming-and-Sea-Ice-Decline, pp. 37–45.

Frey, K. E., J. C. Comiso, L. W. Cooper, J. M. Grebmeier and L. V. Stock, 2019: Arctic Ocean Primary Productivity: The response of marine algae to climate warming and sea ice decline. In: [Arctic Report Card 2019], https://arctic.noaa.gov/Report-Card/Report-Card-2019/ArtMID/7916/ArticleID/839/Arctic-Ocean-Primary-Productivity-The-Response-of-Marine-Algae-to-Climate-Warming-and-Sea-Ice-Decline, pp. 40–47.

Giesbrecht, K. E., D. E. Varela, J. Wiktor, J. M. Grebmeier, B. Kelly and J. E. Long, 2019: A decade of summertime measurements of phytoplankton biomass, productivity and assemblage composition in the Pacific Arctic Region from 2006 to 2016. *Deep Sea Res. Part II Top. Stud. Oceanogr.*, 162, 93–113, doi.org/10.1016/j.dsr2.2018.06.010.

Henley, S. F., M. Porter, L. Hobbs, J. Braun, R. Guillaume-Castel, E. J. Venables, E. Dumont and F. Cottier, 2020: Nitrate supply and uptake in the Atlantic Arctic sea ice zone: seasonal cycle, mechanisms and drivers. *Philos. Trans. Royal Soc. A*, 37820190361. http://doi.org/10.1098/rsta.2019.0361.

Hill, V., M. Ardyna, S. H. Lee, and D. E. Varela, 2018: Decadal trends in phytoplankton production in the Pacific Arctic Region from 1950 to 2012. *Deep Sea Res. Part II Top. Stud. Oceanogr.*, 152, 82–94, doi.org/10.1016/j.dsr2.2016.12.015.

Lalande, C., J. M. Grebmeier, R. R. Hopcroft and S. Danielson, 2020: Annual cycle of export fluxes of biogenic matter near Hanna Shoal in the northeast Chukchi Sea. *Deep Sea Res. Part II Top. Stud. Oceanogr.*, 177, 104730.

Lalande, C., E. -M. Nöthig and L. Fortier, L., 2019: Algal Export in the Arctic Ocean in Times of Global Warming. *Geophys. Res. Lett.*, 46, 5959–5967.

Leu, E., C. J. Mundy, P. Assmy, K. Campbell, T. M. Gabrielsen, M. Gosselin, T. Juul-Pedersen, and R. Gradinger, 2015: Arctic spring awakening – Steering principles behind the phenology of vernal ice algal blooms. *Prog. Oceanogr.*, http://dx.doi.org/10.1016/j.pocean.2015.07.012.

Lewis, K. M., G. L. van Dijken and K. R. Arrigo, 2020: Changes in phytoplankton concentration now drive increased Arctic Ocean primary production. *Science*, 369, 198–202.

Moore, S. E., and J. M. Grebmeier, 2018: The Distributed Biological Observatory: Linking Physics to Biology in the Pacific Arctic Region. *Arctic*, 71, Suppl. 1, 1–7, http://doi.org/10.14430/arctic4606.

Neeley, A. R., L. A. Harris, K. E. Frey (2018), Unraveling phytoplankton community dynamics in the northern Chukchi and western Beaufort seas amid climate change. *Geophys. Res. Lett. 45*, https://doi.org/10.1029/2018GL077684.

Randelhoff, A., L. Lacour, C. Marec, E. Leymarie, J. Lagunas, X. Xing, G. Darnis, C. Penkerc'h, M. Sampei, L. Fortier, F. D'Ortenzio, H. Claustre and M. Babin, 2020: Arctic mid-winter phytoplankton growth revealed by autonomous profilers. *Sci. Adv.*, 6, eabc2678.

Stabeno, P. and S. W. Bell, 2019: Extreme Conditions in the Bering Sea (2017–2018): Record-Breaking Low Sea-Ice Extent. *Geophys. Res. Lett.*, *46*, 8952–8959. https://doi.org/10.1029/2019GL083816.

Tremblay J.-É., L. G. Anderson, P. Matrai, S. Bélanger, C. Michel, P. Coupel, and M. Reigstad, 2015: Global and regional drivers of nutrient supply, primary production and CO_2 drawdown in the changing Arctic Ocean. *Prog. Oceanogr.*, doi:10.1016/j.pocean.2015.08.009.

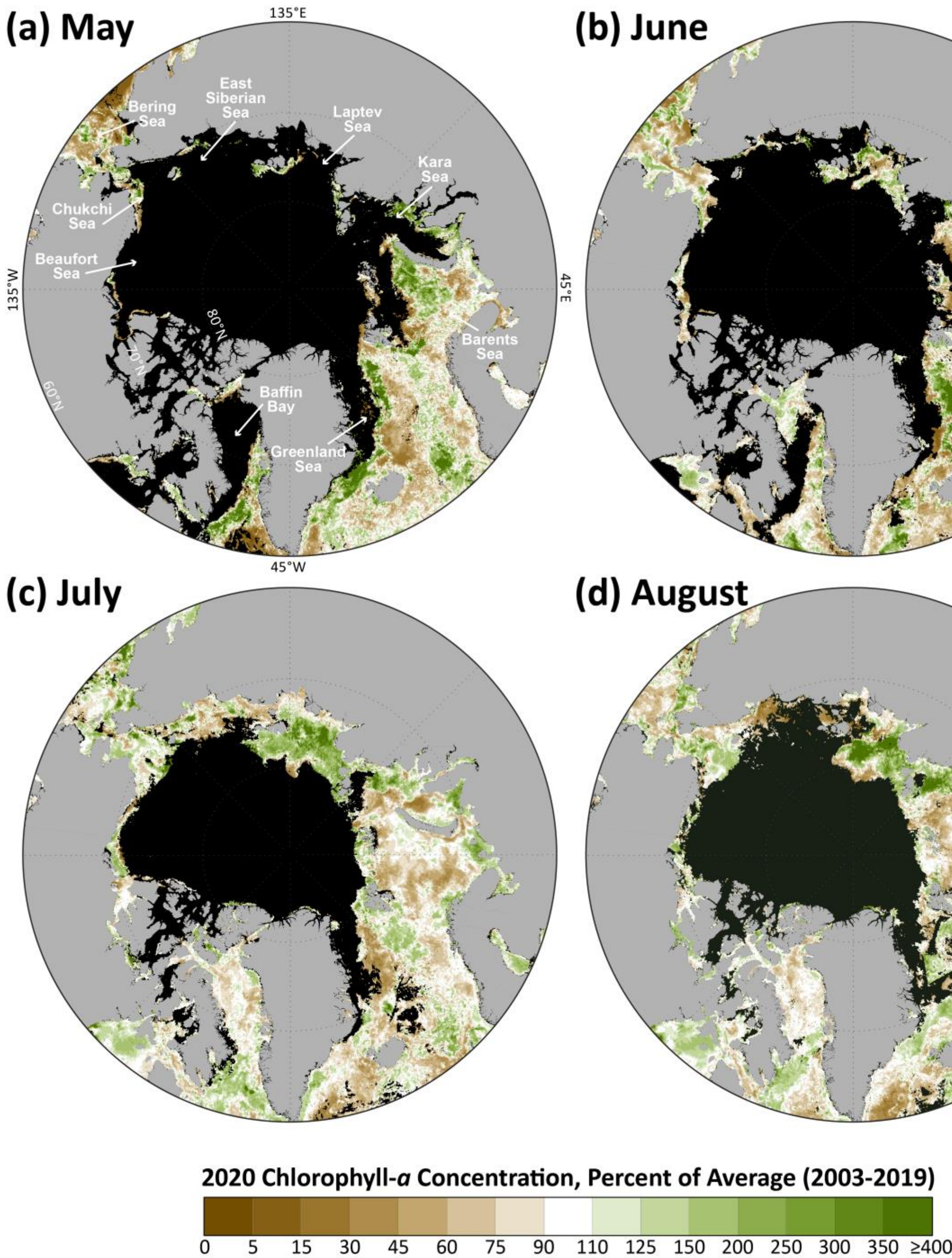

Figure 1. Mean monthly chlorophyll-*a* concentrations during 2020, shown as a percent of the 2003–2019 average for (a) May, (b) June, (c) July, and (d) August. The black regions represent areas where no data are available (owing to either >10% sea ice concentrations or cloud cover). Satellite-based chlorophyll-*a* data across the pan-Arctic region were derived using the MODIS-Aqua Reprocessing 2018.0, chlor_a algorithm: http://oceancolor.gsfc.nasa.gov/.

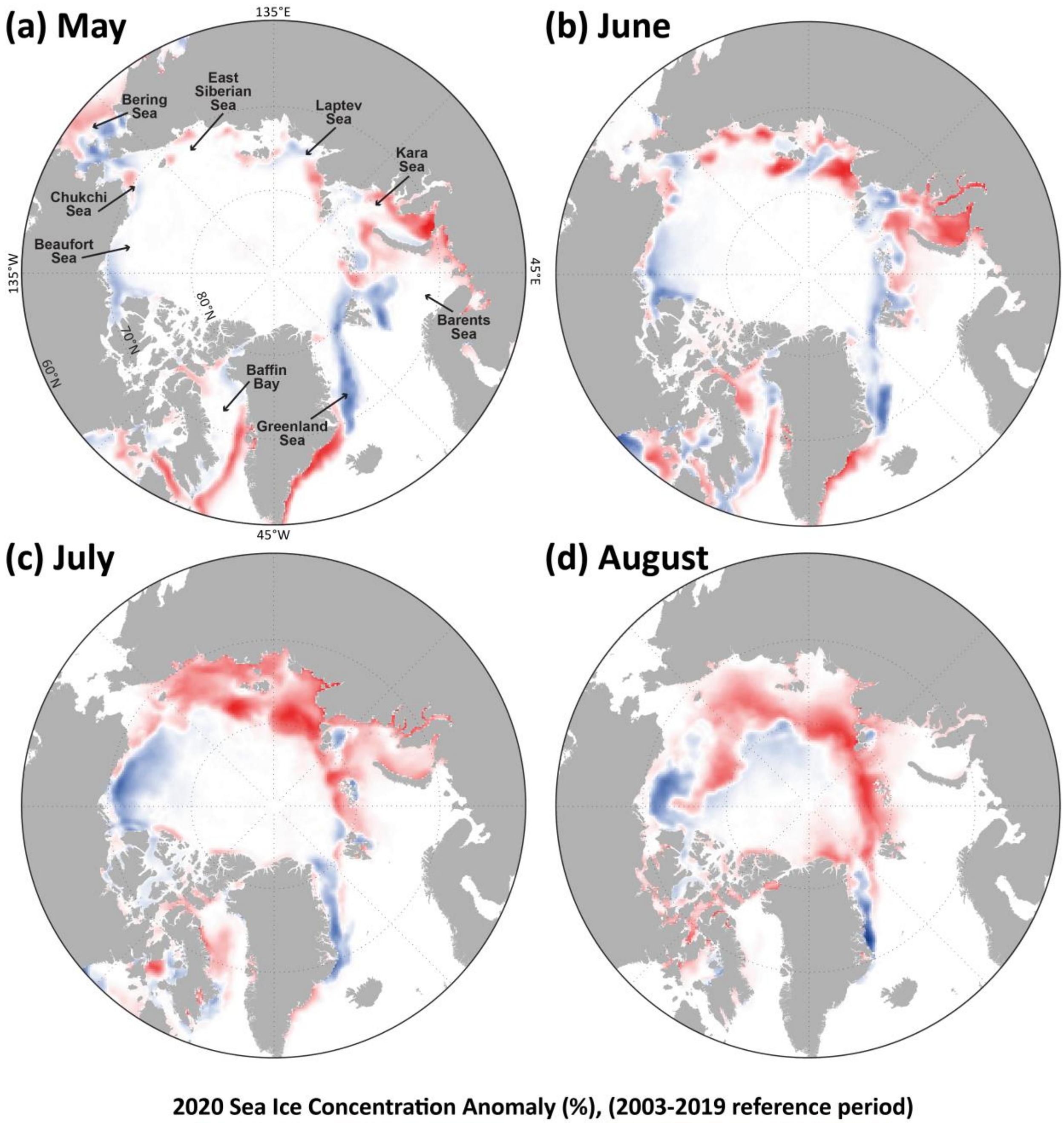

Figure 2. Sea ice concentration anomalies (%) in 2020 (compared to a 2003–2019 mean reference period) for (a) May, (b) June, (c) July, and (d) August. Satellite-based sea ice concentrations were derived from the Special Sensor Microwave/Imager (SSM/I) and Special Sensor Microwave Imager/Sounder (SSMIS) passive microwave instruments, calculated using the Goddard Bootstrap (SB2) algorithm (Comiso et al., 2017a; Comiso et al., 2017b).

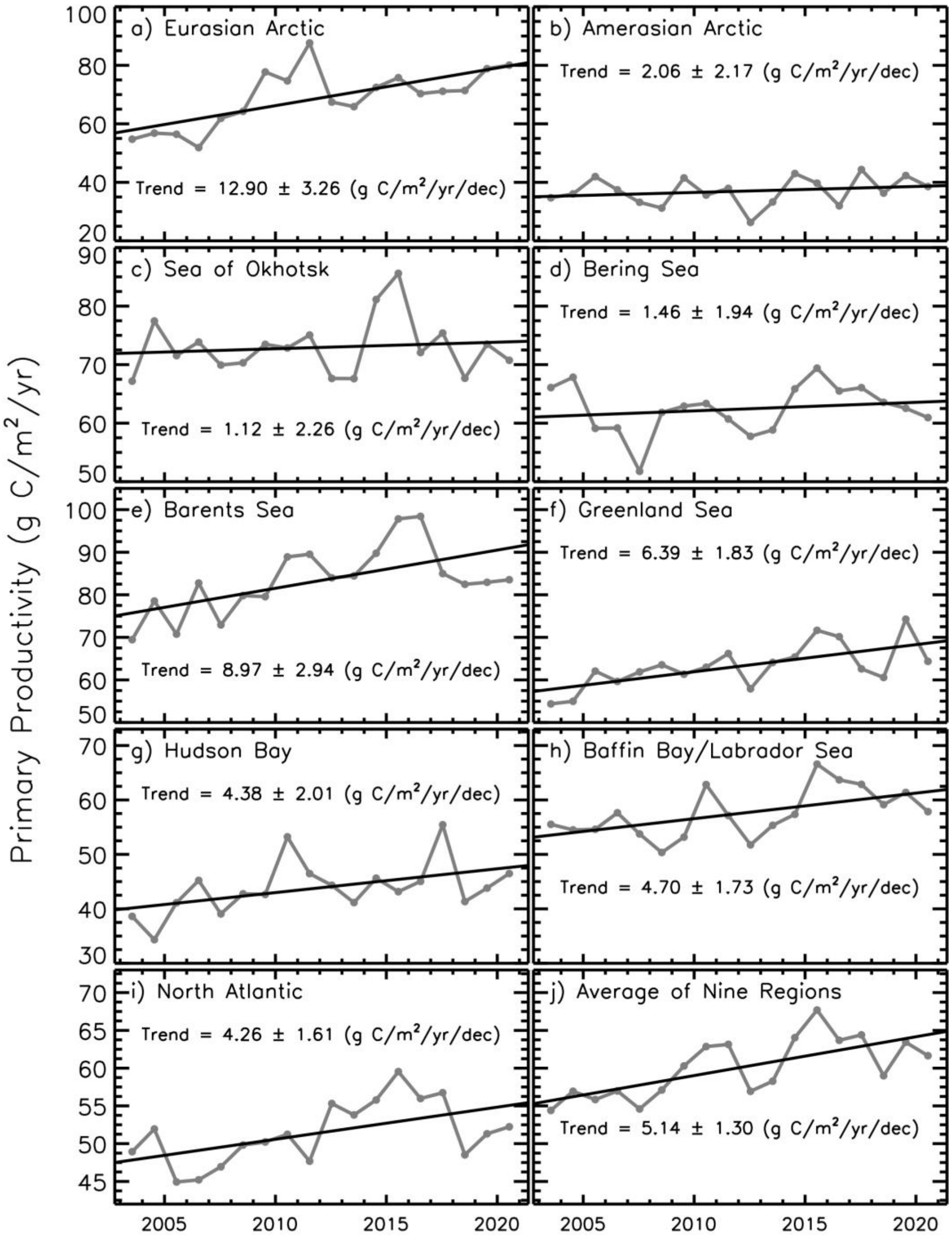

Fig. 3. Primary productivity (2003–2020, March-September only) in nine different regions of the Northern Hemisphere (for a definition of the regions see Comiso, 2015), as well as the average of these nine regions, derived using chlorophyll-*a* concentrations from MODIS-Aqua data, the NOAA 1/4° daily Optimum Interpolation Sea Surface Temperature dataset (or daily OISST) that uses satellite sea surface temperatures from AVHRR, and additional parameters. Values are calculated based on the techniques described by Behrenfeld and Falkowski (1997) and represent net primary productivity (NPP). Additional information regarding these data can be found in **Table 1**.

Table 1. Linear trends, statistical significance, percent change and primary productivity anomalies in 2020 (March-September) in the nine regions (and overall average) as shown in **Fig. 4**. Utilizing the Mann-Kendall test for trend, values in **bold** are significant at the 95% confidence level. The percent change was estimated from the linear regression of the 18-year time series.

Region	**Trend, 2003–2020 ($gC/m^2/yr/decade$)**	**Mann-Kendall *p*-value**	**% Change**	**2020 Anomaly ($g C/m^2/yr$) from a 2003–2019 reference period**	**2020 Primary Productivity (% of the 2003–2019 average)**
Eurasian Arctic	**12.90**	0.000	37.9	11.87	117.4
Amerasian Arctic	2.06	0.293	10.0	1.69	104.6
Sea of Okhotsk	1.12	0.654	2.7	-2.33	96.8
Bering Sea	1.46	0.654	4.1	-1.54	97.5
Barents Sea	**8.97**	0.005	20.1	0.18	100.2
Greenland Sea	**6.39**	0.004	18.8	1.21	101.9
Hudson Bay	**4.38**	0.021	18.5	2.76	106.3
Baffin Bay/Labrador Sea	**4.70**	0.039	14.9	0.34	100.6
North Atlantic	**4.26**	0.007	15.1	0.83	101.6
Average of Nine Regions	**5.14**	0.001	15.7	1.67	102.8